

# Modified UCN2 peptide treatment improves skeletal muscle mass and function in mouse models of obesity-induced insulin resistance

Melissa L. Borg<sup>1</sup>, Julie Massart<sup>2</sup>, Thais De Castro Barbosa<sup>1</sup>, Adrià Archilla-Ortega<sup>1</sup>, Jonathon A.B. Smith<sup>1</sup>, Johanna T. Lanner<sup>3</sup>, Jorge Alsina-Fernandez<sup>4</sup>, Benjamin Yaden<sup>4</sup>, Alexander E. Culver<sup>4</sup>, Håkan K.R. Karlsson<sup>2</sup>, Joseph T. Brozinick<sup>4</sup> & Juleen R. Zierath<sup>1,2\*</sup> 

<sup>1</sup>Department of Physiology and Pharmacology, Section for Integrative Physiology, Karolinska Institutet, Stockholm, Sweden; <sup>2</sup>Department of Molecular Medicine and Surgery, Section for Integrative Physiology, Karolinska Institutet, Stockholm, Sweden; <sup>3</sup>Department of Physiology and Pharmacology, Section for Molecular Muscle Physiology and Pathophysiology, Karolinska Institutet, Stockholm, Sweden; <sup>4</sup>Lilly Research Laboratories, Division of Eli Lilly and Company, Indianapolis, IN, USA

## Abstract

**Background** Type 2 diabetes and obesity are often seen concurrently with skeletal muscle wasting, leading to further derangements in function and metabolism. Muscle wasting remains an unmet need for metabolic disease, and new approaches are warranted. The neuropeptide urocortin 2 (UCN2) and its receptor corticotropin releasing factor receptor 2 (CRHR2) are highly expressed in skeletal muscle and play a role in regulating energy balance, glucose metabolism, and muscle mass. The aim of this study was to investigate the effects of modified UCN2 peptides as a pharmaceutical therapy to counteract the loss of skeletal muscle mass associated with obesity and casting immobilization.

**Methods** High-fat-fed mice (C57Bl/6J; 26 weeks old) and ob/ob mice (11 weeks old) were injected daily with a PEGylated (Compound A) and non-PEGylated (Compound B) modified human UCN2 at 0.3 mg/kg subcutaneously for 14 days. A separate group of chow-fed C57Bl/6J mice (12 weeks old) was subjected to hindlimb cast immobilization and, after 1 week, received daily injections with Compound A. *In vivo* functional tests were performed to measure protein synthesis rates and skeletal muscle function. *Ex vivo* functional and molecular tests were performed to measure contractile force and signal transduction of catabolic and anabolic pathways in skeletal muscle.

**Results** Skeletal muscles (*extensor digitorum longus*, *soleus*, and *tibialis anterior*) from high-fat-fed mice treated with Compound A were ~14% heavier than muscles from vehicle-treated mice. Chronic treatment with modified UCN2 peptides altered the expression of structural genes and transcription factors in skeletal muscle in high-fat diet-induced obesity including down-regulation of *Trim63* and up-regulation of *Nr4a2* and *Igf1* ( $P < 0.05$  vs. vehicle). Signal transduction via both catabolic and anabolic pathways was increased in *tibialis anterior* muscle, with increased phosphorylation of ribosomal protein S6 at Ser<sup>235/236</sup>, FOXO1 at Ser<sup>256</sup>, and ULK1 at Ser<sup>317</sup>, suggesting that UCN2 treatment modulates protein synthesis and degradation pathways ( $P < 0.05$  vs. vehicle). Acutely, a single injection of Compound A in drug-naïve mice had no effect on the rate of protein synthesis in skeletal muscle, as measured via the surface sensing of translation method, while the expression of *Nr4a3* and *Ppargc1a4* was increased ( $P < 0.05$  vs. vehicle). Compound A treatment prevented the loss of force production from disuse due to casting. Compound B treatment increased time to fatigue during *ex vivo* contractions of fast-twitch *extensor digitorum longus* muscle. Compound A and B treatment increased lean mass and rates of skeletal muscle protein synthesis in ob/ob mice.

**Conclusions** Modified human UCN2 is a pharmacological candidate for the prevention of the loss of skeletal muscle mass associated with obesity and immobilization.

**Keywords** Muscle wasting; Obesity; Diabetes; Insulin resistance; Exercise; Therapy

Received: 9 February 2021; Revised: 25 May 2021; Accepted: 8 June 2021

\*Correspondence to: Prof. Juleen R. Zierath, Department of Molecular Medicine and Surgery, Section for Integrative Physiology, Karolinska Institutet, Biomedicum C4, Solnavägen 9, SE 171 77 Stockholm, Sweden. Tel: +46 (0) 8-524 875 80, Email: juleen.zierath@ki.se

With the advent of western diets rich in saturated fat and a greater incidence of sedentary lifestyles, the incidence of obesity in the world population is reaching unprecedented levels.<sup>1</sup> Obesity can lead to several co-morbidities such as insulin resistance, type 2 diabetes mellitus, hypertension, cardiovascular disease, osteoarthritis, and certain cancers. Retention of lean muscle mass is crucial for the maintenance of insulin sensitivity and overall metabolic health.<sup>2,3</sup> A co-morbidity of long-term obesity is the loss of skeletal muscle mass, which points to the importance of lean muscle mass for maintenance of metabolic health.<sup>4</sup> While controversial, loss of muscle mass in obesity can be prevented and perhaps reversed with medicine and/or lifestyle changes such as diet and exercise. Whether due to a lack of compliance or lack of mobility amongst the morbidly obese, lifestyle interventions are unlikely to succeed as a long-term strategy against the loss of skeletal muscle mass, requiring suitable pharmacological interventions.

During obesity and related muscle atrophy disorders, skeletal muscle mass and its metabolic and functional properties are impaired. Numerous mechanisms have been implicated in skeletal muscle wasting associated with disease, including neuronal,<sup>5</sup> hormonal,<sup>6</sup> nutritional,<sup>7</sup> lack of physical activity,<sup>8</sup> and low-grade inflammation.<sup>9</sup> Muscle wasting is characterized by decreases in fiber size, concomitant with a fiber type switch, and preferential loss of type II glycolytic fibers. Reductions in protein synthesis and mitochondrial function, as well as intramuscular contractile dysfunction, are also features of this condition.<sup>4,5</sup> Nonetheless, a modest gain in skeletal muscle mass has a vast impact on whole-body metabolism and prevents the development of insulin resistance and obesity.<sup>4,10</sup>

Members of the corticotropin releasing factor (CRF) family [CRF, urocortin (UCN) 1, 2, and 3]<sup>11</sup> signal through two different G protein-coupled receptors (CRHR1 and 2).<sup>12</sup> These 38–41 amino acid peptides are structurally related and are differentially expressed throughout the central nervous system and peripheral tissues,<sup>11,12</sup> where they play a role in modulating the hypothalamic–pituitary–adrenal axis.<sup>13</sup> CRHR2 is activated by UCN1, 2, and 3, while CRHR1 is activated by CRF and UCN1. CRHR2 and its ligand, UCN2, are highly expressed in skeletal muscle.<sup>14–16</sup> UCN2 and CRHR2 play a role in modulating skeletal muscle growth and metabolism. CRHR2 expression is increased in skeletal muscle of high-fat-fed mice,<sup>17</sup> while CRHR2-knockout mice are resistant to high-fat diet (HFD)-induced fat accumulation and insulin resistance.<sup>18</sup> Recent data have shown that UCN3 transgenic mice have increased skeletal muscle mass with myocyte hypertrophy and are protected from obesity.<sup>19</sup> Loss of skeletal muscle mass and function from nerve damage, corticosteroids, or disuse is prevented by sauvagine, a selective CRHR2 agonist, or human UCN2 in rodents.<sup>20–22</sup> Furthermore, in lean rodents, human UCN2 administration causes skeletal muscle hypertrophy.<sup>20,21</sup> The CRHR2 receptor is also involved in

modulating skeletal muscle growth in chronic muscle wasting disorders. Treating mdx mice (a model for Duchenne muscular dystrophy) with a CRHR2 agonist prevents the progressive degeneration of diaphragm muscle,<sup>23</sup> while treatment with CRHR2 agonists in models of aging or chronic heart failure in rats and emphysema in hamsters improves skeletal muscle mass and power output.<sup>24</sup> Activating CRHR2 modulates hypertrophy and skeletal muscle function in a variety of models with acute or chronic pathologies. The effects of chronic activation of CRHR2 on skeletal muscle function, growth, and metabolism in obesity are unknown.

We have reported that treatment of insulin-resistant obese mice with a PEGylated peptide of human UCN2 resulted in a 10% loss of body weight and improved whole-body glucose homeostasis.<sup>25</sup> This was attributed to a direct insulin sensitizing effect of UCN2 on skeletal muscle.<sup>25</sup> Given that UCN2 peptides and CRHR2 agonists modulate skeletal muscle metabolism and hypertrophy, we hypothesized that UCN2 treatment will increase skeletal muscle mass and functional properties in models of insulin resistance and obesity. We investigated the effects of two modified UCN2 peptides in the regulation of skeletal muscle mass and function in diet-induced obesity and leptin-deficient ob/ob mice, as well as in preserving muscle function during casting immobilization.

## Methods

### Peptide synthesis

Modified human UCN2 peptides (Compounds A and B) are based on the previously reported Compound 8<sup>26</sup> and synthesized using established solid-phase peptide synthesis protocols as described.<sup>25,26</sup> While Compound B corresponds to the Compound 8, Compound A has a further modification, with a cystine residue at position 29, where a polyethylene glycol (PEG) 20 000 is attached through an acetamide-base linker. Formulated aliquots of the peptides in phosphate-buffered saline were stored at  $-20^{\circ}\text{C}$ . Working solutions were freshly prepared from thawed stock aliquots diluted with 0.5% Lactoalbumin/0.9% sterile isotonic NaCl.

### Pharmacokinetics

The pharmacokinetic properties of Compound A have been described<sup>25</sup> and have a half-life of 22.3 h. The pharmacokinetic properties of Compound B have been described<sup>26</sup> and result in a considerably shorter half-life of ~30 min.

## Animal care and husbandry

All animal studies have been approved by the appropriate ethics committee and have been performed in accordance with the ethical standards laid down in the 1964 Declaration of Helsinki and its later amendments. Experiments were approved by the Stockholm North Animal Ethical Committee or the Eli Lilly Institutional Animal Care and Use Committee. Male mice (C57Bl/6J) were purchased from Charles River Laboratories (Sulzfeld, Germany) or Envigo (Somerset, USA) at 5 weeks of age. Mice were maintained under a 12 h light/dark cycle in humidity and temperature-controlled environment and had free access to water and standard rodent chow (4% kcal from fat, R34; Lantmännen, Kimstad, Sweden). At 6 weeks of age, mice were either placed on a standard rodent chow or HFD (60% kcal from fat, TD.06414, Harlan Laboratories) *ad libitum* for 20 weeks. Mice were single housed after 19 weeks on HFD. After 20 weeks on HFD, mice received daily subcutaneous injections of vehicle, Compound A, or Compound B at 0.3 mg/kg of body weight for 14 days before the onset of the dark period. Injections were performed in the intrascapular region and hind leg on alternating days to minimize discomfort. Total lean mass was assessed in conscious mice using the EchoMRI-100 system (Echo Medical Systems). Separate experiments were conducted using male *ob/ob* mice (B6.V-Lepob/*ob*/JRj; Janvier Labs, Le Genest St. Isle, France) at 10 weeks of age. *Ob/ob* mice exhibit loss of skeletal muscle mass and are a model of hyperinsulinemia, insulin resistance, and morbid obesity due to leptin deficiency.<sup>27,28</sup> Mice were group housed (three per cage) and had free access to standard rodent chow (3.36% kcal from fat, CRM, Special Diet Services). At 11 weeks of age, mice received daily subcutaneous injections of vehicle, Compound A, or Compound B at 0.3 mg/kg of body weight for 14 days. Total fat and lean mass was assessed using the EchoMRI-100 before the start of injections and at Day 12 of the injections.

## Free wheel running

After 19 weeks on HFD, mice were randomized into sedentary and wheel running groups as described,<sup>25</sup> for 14 days during the treatment period.

## In vivo protein synthesis

Surface sensing of translation (SUnSET) was performed to assess Compound A-induced and B-induced protein synthesis *in vivo* as described.<sup>29</sup> Drug-naïve 20-week-old mice on a standard rodent chow diet received a single subcutaneous injection of vehicle, Compound A, or Compound B at 0.3 mg/kg of body weight. Mice were injected intraperitoneally with

0.04  $\mu\text{mol/g}$  body weight of puromycin (Sigma-Aldrich) dissolved in phosphate-buffered saline 3.5 h after Compound A injection or 30 min after Compound B and vehicle injections (Figure 4A). These times were chosen based on the time to maximal plasma concentration of the drug after subcutaneous injection. Food was removed from all mice once Compound A was injected (4 h fast all together). Tissues were collected 30 min after the puromycin injection and directly snap frozen. Tissue homogenates were prepared in lysis buffer, and 15  $\mu\text{g}$  of protein was used for western blot analysis with an anti-puromycin antibody (12D10; Millipore). Protein synthesis rates were estimated by puromycin incorporation into protein determined by quantifying the immunoreactive bands for each sample, normalized to the ponceau stain. In a separate analysis, SUnSET was also performed in *ob/ob* mice. Mice underwent 14 days of treatment with vehicle, Compound A, and Compound B as described earlier. On Day 14 of the treatment, mice received a final subcutaneous injection and subsequently an intraperitoneal injection of 0.04  $\mu\text{mol/g}$  body weight of puromycin 3.5 h after the Compound A injection or 30 min after the Compound B and vehicle injections. Food was removed from all mice once Compound A was injected (4 h fast in total). Tissues were collected 30 min after puromycin injection and snap frozen.

## Hindlimb cast immobilization

Male C57Bl/6J mice were purchased at 10 weeks of age from Harlan (Indianapolis, USA). Mice were maintained under a 12 h light/dark cycle in humidity and temperature-controlled environment and had free access to water and standard rodent chow (Diet 2014 with 0.95% Ca and 0.67% P, Teklad, Madison, WI). At 12 weeks of age, mice were placed under isoflurane anesthesia, one hindlimb was shaved, and casting was placed on the lower limb in the plantarflexed position (Vet-Lite casting; Jorgensen Laboratories, Loveland, CO). At this time, sham animals were briefly anesthetized and shaved. All mice were individually housed, and casts were replaced every 7 days to ensure continual immobilization.

## In situ skeletal muscle function after casting

After 1 week of hindlimb cast immobilization, the mice received daily subcutaneous injection of vehicle or Compound A as described earlier for 14 days. After the treatment on Day 15, non-fasted mice were anesthetized with isoflurane, the cast was removed and hindlimb shaved, the knee was clamped with a blunted set screw, and the foot was secured in a foot pedal using the 807B *In situ* Large Rodent/Small Animal Apparatus (Aurora, ON, Canada). Gastrocnemius muscle contractions were induced by directly

stimulating the tibial nerve with two electrodes. To determine the optimal resting length of the muscle (LO), single twitches were applied at different muscle lengths. Thereafter, experimental tetanic/twitch protocols were performed, the force of the contracting muscle was recorded, and strength and fatigue were measured. Mice were then killed, and muscles dissected and weighed.

### Gene expression analysis after casting

In a separate cohort of mice, the hindlimb was cast immobilized for 14 days; thereafter, the mice received a single dose of 0.3 mg/kg Compound A or vehicle administered subcutaneously. Six hours later, non-fasted mice were sacrificed, and tissues were harvested and snap frozen in liquid nitrogen. RNA was extracted from frozen muscle tissues as described in the succeeding text. qPCR was performed with TaqMan Fast Advance Master Mix (Thermo Fisher Scientific) with the ABI Prism 7900HT system (Applied Biosystems). The Taqman primer probes are listed in Supporting Information, Table S1 (Thermo Fisher Scientific).

### Contraction-induced glucose uptake

Mice were fed with HFD for 19 weeks and then single housed for 1 week prior to randomization into the following treatment groups: vehicle ( $n = 10$ ), Compound A ( $n = 10$ ), or Compound B ( $n = 10$ ) treatment. Vehicle-treated mice fed with a standard chow diet ( $n = 6$ ) were included as a control for the HFD. At the end of the 14 day treatment period, basal and contraction-induced glucose uptake was assessed in *extensor digitorum longus* (EDL) muscle as described.<sup>30</sup> Mice were fasted for 4 h and anesthetized via an intraperitoneal injection of 2.5% Avertin [2,2,2-tribromo ethanol and tertiary amyl alcohol (16  $\mu\text{L/g}$  body weight)]. Paired EDL muscles were placed at resting passive tension (4–5 mN) for 20 min in contraction chambers (Muscle Strip Myograph System; Danish Myo Technology, Denmark) containing pre-oxygenated (95%  $\text{O}_2$ /5%  $\text{CO}_2$ ) Krebs–Henseleit buffer supplemented with 5 mM glucose, 15 mM mannitol, 0.3 mM palmitate, and 4% fatty acid-free bovine serum albumin. Then fatigue-inducing contractions were produced by electrical stimulation with 100 Hz (0.2 ms pulse duration, 20 V) at a rate of 0.2 s contraction every 2 s for 10 min, while contralateral EDL muscles were kept under resting passive tension conditions. Raw data were extracted from LabChart files containing recordings of the contraction experiments. After the contraction protocol, EDL muscles were immediately transferred to new vials containing pre-oxygenated Krebs–Henseleit buffer supplemented with 19 mM mannitol, 1 mM 2-deoxy-D-glucose, 2.5  $\mu\text{Ci/mL}$  [ $^3\text{H}$ ]2-deoxy-D-glucose (American Radiolabeled Chemicals), and 0.7  $\mu\text{Ci/mL}$  [ $^{14}\text{C}$ ]

mannitol (Moravek Biochemicals) and incubated for 20 min to assess glucose uptake as described.<sup>31</sup> All *in vitro* skeletal muscle testing was performed at 30°C. Results are expressed as  $\mu\text{M}$  glucose  $\times$  mg protein $^{-1} \times 20$  min $^{-1}$ .

### Biochemical analysis

Glycogen content in the *tibialis anterior* (TA) muscle was measured in 4 h fasted mice using a Glycogen Assay Kit (ab65620; Abcam) according to the manufacturer's protocol. Protein was extracted using lysis buffer [20 mM Tris-HCl pH 7.8, 137 mM NaCl, 2.7 mM KCl, 1 mM MgCl, 10 mM NaF, 1% Triton X-100, 10% glycerol, 1 mM EDTA, 0.5 mM  $\text{NaVO}_3$ , 1 mM PMSF, 1 $\times$  Protease Inhibitor Cocktail (Millipore)], and concentration was determined using a Pierce<sup>™</sup> BCA Protein Assay Kit (#23225, Thermo Fisher Scientific).

### RNA extraction and gene expression analysis

RNA was extracted from the tissues using the Trizol-chloroform method (Invitrogen). cDNA was produced from 1 to 2  $\mu\text{g}$  of RNA using a High-Capacity cDNA Reverse Transcription Kit (Thermo Fisher Scientific). RT-qPCR was performed in duplicate with the use of Fast SYBR Green Master Mix (Thermo Fisher Scientific) with 15 ng cDNA in a 10  $\mu\text{L}$  reaction with a ViiA 7 Real-Time PCR System (Thermo Fisher Scientific). Gene expression was quantified with the  $\Delta\Delta\text{Ct}$  method using the geometric mean of two housekeeping genes as control. Primer details are reported in Table S1.

### Western blot analysis

Western blot analysis was performed as described.<sup>32</sup> Equal amounts of protein (15–20  $\mu\text{g}$ ) were separated by sodium dodecyl sulfate–polyacrylamide gel electrophoresis using Criterion XT Precast gels (Bio-Rad) and transferred to polyvinylidene difluoride membrane (Immobilon-P, Millipore; Billerica, MA). Primary antibodies are reported in Table S2. Bands were quantified using Quantity One 1-D analysis software (Bio-Rad) and normalized to total protein staining with Ponceau S (Sigma Aldrich, St. Louis, MO).

### Statistics

Data are presented as box and whiskers plots; the box extends from the 25th to 75th percentiles with the median indicated; and the whiskers and outliers are plotted using the Tukey method. Normality was verified using the Shapiro–Wilk test. When data were normally distributed, a one-way analysis of variance with Dunnett's multiple

comparison test was used. For data not normally distributed, the Kruskal–Wallis test with Dunn’s multiple comparison was used. Two-way or two-way repeated measures analysis of variance with Sidak’s multiple comparison was also used when necessary. Chow-fed mice were excluded from statistical analysis as they only served as a control for the HFD. Comparisons were considered significant at  $P < 0.05$ . Analyses were performed using GraphPad 8 (GraphPad Software Inc.).

## Results

### *Chronic treatment with modified UCN2 peptides increases skeletal muscle mass in high-fat diet-induced obesity*

Skeletal muscle hypertrophy is enhanced by UCN2 treatment in different models of disuse and immobilization.<sup>33</sup> We assessed total lean mass and skeletal muscle mass in HFD-fed mice after a 14 day treatment with modified UCN2 peptides with or without free access to running wheels. Mice fed a HFD for 20 weeks developed obesity, with hyperinsulinemia, glucose intolerance, and skeletal muscle insulin resistance<sup>25</sup> and reduced skeletal muscle weight relative to body weight (Table S3). Total lean mass tended to increase with Compound A treatment (Figure 1A) and was significantly increased with both Compound A and B treatment when expressed as a percentage of total body weight (Figure 1B). Skeletal muscle mass expressed as either absolute value or a percentage of final body weight was consistently increased in response to Compound A treatment (Figure 1). Specifically, the mass of EDL (Figure 1C and 1D) (primarily glycolytic fibers), soleus (Figure 1E and 1F) (primarily oxidative fibers), and TA (Figure 1G and 1H) (mixed fiber type) was increased in Compound A-treated HFD-fed mice. The mass of soleus muscle was also increased in Compound B-treated HFD-fed mice when expressed as a percentage of final body weight (Figure 1F). Compound A treatment decreased fat mass expressed as either absolute values<sup>25</sup> or percentage of final body weight ( $37.83 \pm 1.11$  vs.  $28.39 \pm 1.31$  g for vehicle vs. Compound A treatment, respectively,  $P < 0.05$ ). Similarly, Compound B treatment decreased fat mass expressed as either absolute values ( $18.86 \pm 0.89$  vs.  $16.81 \pm 0.97$  g for vehicle vs. Compound B treatment, respectively,  $P < 0.05$ ) or percentage of final body weight ( $37.83 \pm 1.11$  vs.  $34.93 \pm 1.36$  for vehicle vs. Compound B treatment, respectively,  $P < 0.05$ ).

To examine the synergistic interaction between UCN2 treatment and physical activity on skeletal muscle mass, HFD-fed mice were given free access to running wheels over the duration of the 14 day treatment period. In vehicle-treated mice, wheel running had no effect on total lean mass and skeletal muscle mass as compared with

vehicle-treated sedentary mice (Figure 1A–1H). Skeletal muscle mass of EDL, soleus, and TA was increased in Compound A versus vehicle-treated mice given free access to running wheels (Figure 1C–1H). Furthermore, there was a synergistic effect between wheel running and Compound A treatment to increase soleus muscle weight as compared with sedentary Compound A-treated mice (Figure 1E and 1F). Wheel running increased soleus mass in Compound B-treated mice as compared with vehicle-treated mice, but only when expressed as a percentage of body weight (Figure 1F). Furthermore, there was a synergistic effect between wheel running and Compound B treatment to increase EDL (Figure 1D) and soleus (Figure 1F) muscle weight as compared with sedentary Compound B-treated mice. The average running distance over the 14 day treatment period was unaltered by either Compound A or Compound B ( $4369 \pm 984$ ,  $3117 \pm 738$ , and  $3993 \pm 854$  m per night for vehicle, Compound A, and Compound B treatment, respectively, not significant). These results indicate a 14 day treatment of HFD-fed mice with modified UCN2 peptides increases skeletal muscle mass in glycolytic, oxidative, and mixed muscle fiber types.

### *Chronic treatment with modified UCN2 peptides alters the expression of structural genes and transcription factors in skeletal muscle in high-fat diet-induced obesity*

We next sought to identify the molecular mechanisms for the increase in skeletal muscle mass with UCN2 treatment by analysing relevant mediators of anabolic and catabolic pathways. The TA muscle was chosen for this analysis as it is a mixed fiber type and was frozen immediately after dissection, whereas the EDL and soleus were incubated *ex vivo* and used to assess force production and glucose metabolism.<sup>25</sup> mRNA analysis of genes associated with muscle function and growth suggests that Compound A treatment resulted in a fiber type transformation, with decreased expression of *Myh2* [which codes for myosin heavy chain (MHC) 2A] and a trend for decreased *Myh7* (MHC $\beta$ ), associated with oxidative characteristics, and a concomitant increase in *Myh1* (MHC2X) expression, and a trend for increased *Myh4* (MHC2B) expression, associated with glycolytic fast-twitch fibers (Figure 2A). While the ‘gold standard’ of measuring fiber type composition (histological staining) was not performed in this study, gene expression analysis is suggestive of a fiber type switch from oxidative to glycolytic fibers in the TA from Compound A-treated mice. Furthermore, Compound B treatment decreased the expression of *Trim63*, which codes for MuRF1, an E3 ubiquitin ligase important for skeletal muscle remodelling (Figure 2B), whereas both Compound A and B treatment increased expression of the growth factor *Igf1* (Figure 2C). In addition, Compound A treatment increased *Nr4a2* expression, and Compound B treatment

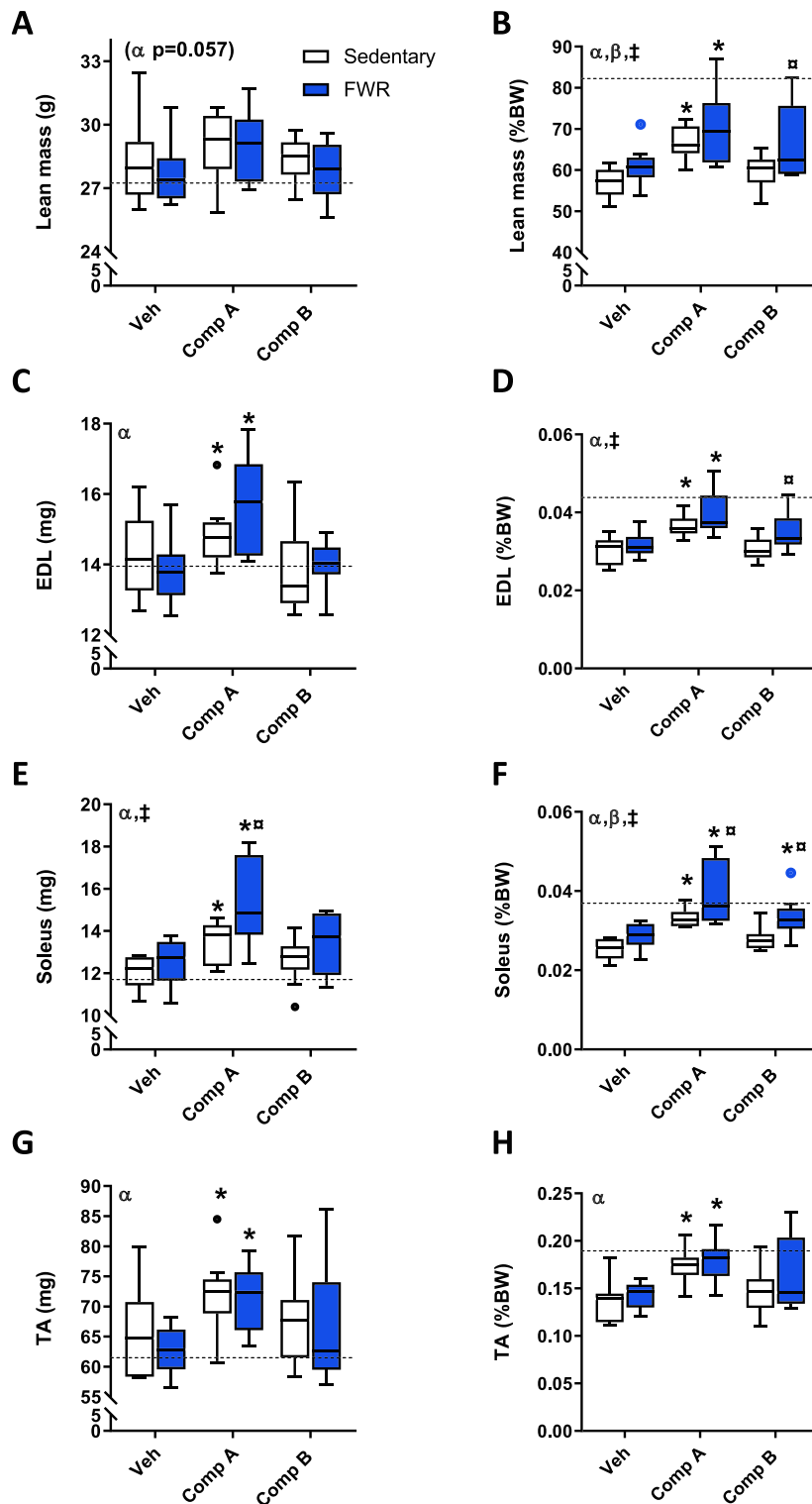


**Figure 1** UCN2 treatment increases skeletal muscle mass in HFD-fed mice. High-fat diet (HFD)-fed mice were either sedentary or had access to free wheel running (FWR) and treated with vehicle, Compound A, or Compound B for 14 days. Lean mass was assessed with EchoMRI and expressed as (A) absolute values and (B) a percentage of body weight. Absolute weight of the (C) *extensor digitorum longus* (EDL) and (D) presented as a percentage of body weight. Absolute weight of the (E) soleus and (F) presented as a percentage of body weight. Absolute weight of the (G) *tibialis anterior* (TA) and (H) presented as a percentage of body weight. Dotted line indicates mean of chow vehicle mice.  $n = 9\text{--}10$  mice per group.  $\alpha$ Main effect for Compound A treatment.  $\beta$ Main effect for Compound B treatment.  $\ddagger P < 0.05$  main effect for wheel running. \*Compared with vehicle of same condition.  $\ddagger$ Compared with corresponding sedentary of same treatment as assessed via two-way analysis of variance with Sidak's *post hoc* analysis.

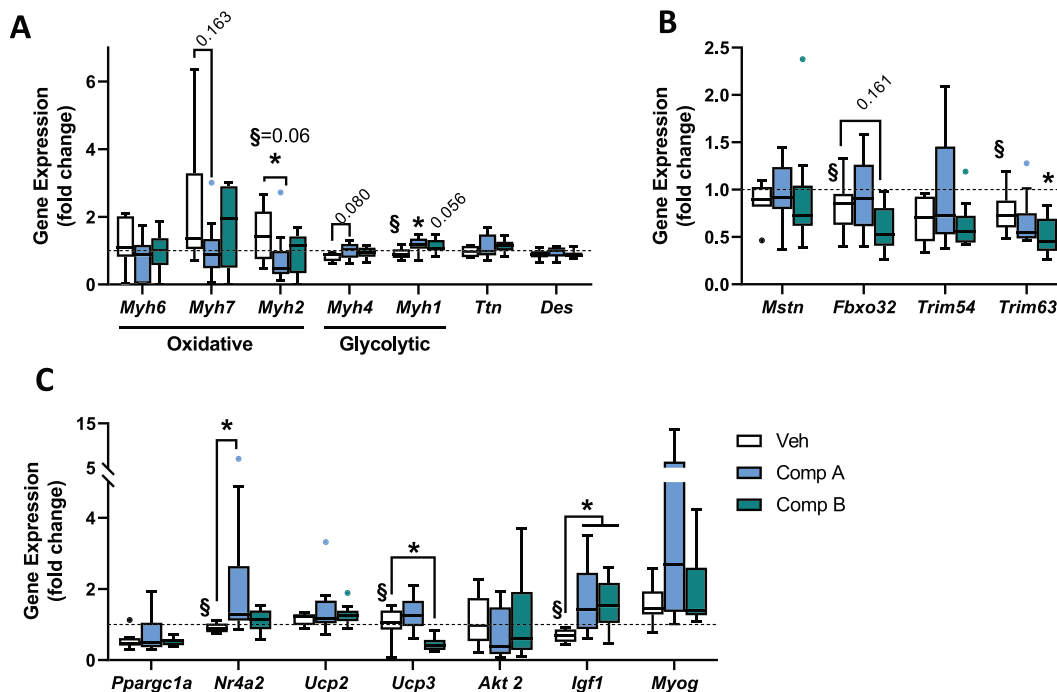


**Figure 2** UCN2 treatment affects genes that are mediators of skeletal muscle hypertrophy and degradation in HFD-fed mice. Effects of Compound A or B treatment on relative mRNA expression of key mediators in pathways regulating muscle mass. Gene expression data were assessed via qPCR analysis of mRNA from the *tibialis anterior* (TA) after high-fat feeding and 14 days of Compound A or B treatment. (A) Genes of thick filaments and structural proteins. (B) Genes and transcription factors involved in protein degradation. (C) Genes and transcription factors involved in hypertrophy. Dotted line indicates the mean of chow vehicle mice. Results are expressed relative to chow vehicle-treated mice and normalized to the geometric mean of *B2M* and *Tbp*.  $n = 8$ – $10$  mice per group. § $P < 0.05$  effect as assessed via one-way analysis of variance or Kruskal–Wallis test, \* $P < 0.05$  versus vehicle as assessed via *post hoc* analysis.

down-regulated expression of the lipid accumulation protective gene *Ucp3* (Figure 2C). These results collectively suggest that UCN2 treatment triggers a change in fiber type composition in skeletal muscle, with down-regulation of *Trim63* and up-regulation of *Nr4a2* and *Igf1*.

### Chronic treatment with modified UCN2 peptides affects proteins that are mediators of skeletal muscle hypertrophy and degradation in high-fat diet-induced obesity

To further elucidate the molecular mechanisms for increased skeletal muscle mass after UCN2 treatment, we analysed the abundance and phosphorylation status of proteins involved in pathways controlling catabolic and anabolic processes. While Compound B was without effect, western blot analysis revealed a trend for increased AKT phosphorylation at Ser<sup>473</sup> and total AKT abundance (Figure 3A) in skeletal muscle from Compound A-treated mice. Phosphorylation of ribosomal protein S6 at Ser<sup>235/236</sup> was increased with levels restored to normal chow levels (Figure 3B), suggesting that Compound A treatment increases mRNA translation. FOXO1 phosphorylation at Ser<sup>256</sup> was increased by both Compound A and B treatment (Figure 3C), suggesting that its transcriptional activity would be inhibited, resulting in suppressed

expression of pro-atrophic E3 ubiquitin ligases.<sup>34</sup> Surprisingly, content of MAFbx was increased after Compound A treatment and restored to normal chow levels (Figure 3C). Furthermore, phosphorylation of ULK1 at Ser<sup>317</sup> was increased above both chow and HFD vehicle levels after Compound A treatment, while AMPK $\alpha$  phosphorylation at Thr<sup>172</sup> tended to increase (Figure 3D), indicating the activation of autophagy. Collectively, these results suggest that UCN2 treatment modulates protein synthesis and degradation pathways, ultimately resulting in increased skeletal muscle mass.

### Modified UCN2 peptides acutely increase transcriptional activity in skeletal muscle from chow-fed mice

Our results provide a snapshot of gene transcription and protein signaling events in skeletal muscle ~16 h after the last treatment with UCN2 peptides. We next sought to directly measure rates of protein synthesis and gene transcription after a single injection of Compound A or B. Protein synthesis was measured by analysing the amount of puromycin incorporated into newly synthesized proteins using the SUnSET method<sup>29</sup> (Figure 4A). Neither Compound A nor B injection acutely altered the rates of protein synthesis in the EDL, soleus, or TA muscle (Figure 4B).

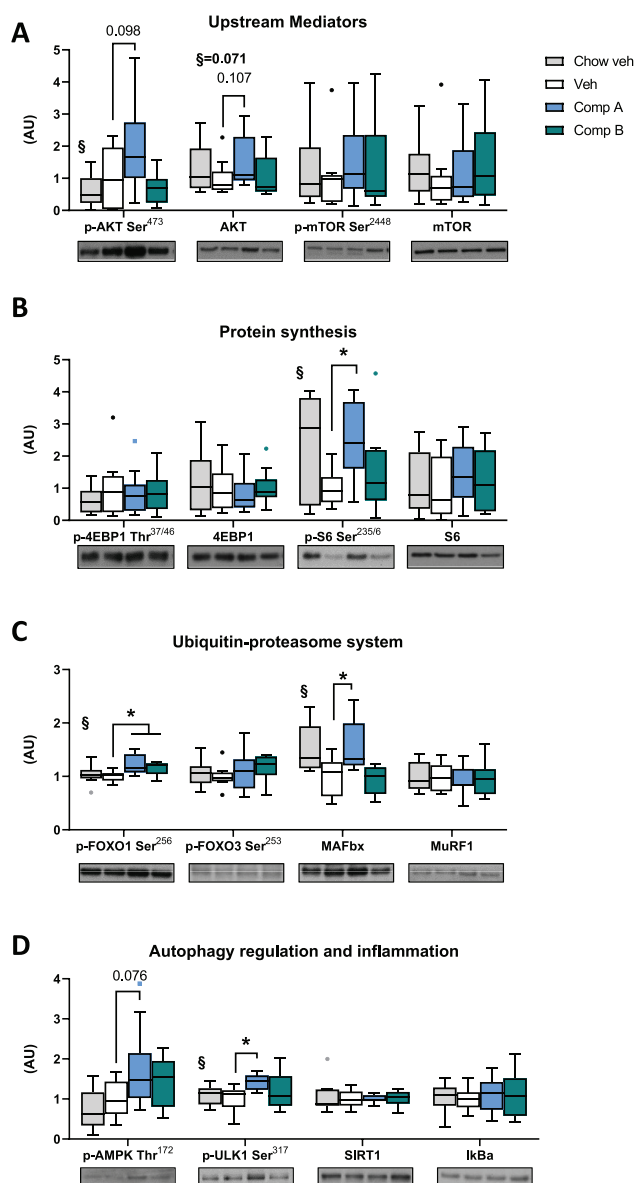


**Figure 3** UCN2 treatment affects proteins that are mediators of skeletal muscle hypertrophy and degradation in HFD-fed mice. Effects of Compound A or B treatment on protein content and phosphorylation of key mediators in pathways regulating muscle mass assessed via western blot analysis of *tibialis anterior* (TA) after high-fat feeding and 14 days of Compound A or B. (A) Upstream mediators in muscle mass regulation. (B) Proteins involved in hypertrophy and protein synthesis. (C) Proteins involved in ubiquitin-proteasome system for protein breakdown. (D) Proteins involved in autophagy regulation and inflammation. Results calculated relative to ponceau stain and expressed relative to HFD vehicle-treated mice.  $n = 8-10$  mice per group.  $^{\S}P < 0.05$  effect as assessed via one-way analysis of variance or Kruskal–Wallis test,  $*P < 0.05$  versus vehicle as assessed via *post hoc* analysis.

Acute injection of Compound A or B did not alter the expression of structural protein genes in TA muscle (Figure 4C), whereas a decrease in pro-atrophy *Fbxo32* (*MAFbx*) and an increase in *Trim63* (*MuRF1*) were observed

with acute Compound A injection (Figure 4D). While Compound B was without effect, acute Compound A injection increased the expression of *Ppargc1a* (*PGC1 $\alpha$* ), *Ppargc1a4* (*PGC1 $\alpha$ 4*), *Nr4a2*, *Nr4a3*, *Ucp3*, and *Myog*, genes also regulated by exercise (Figure 4E). These results in TA muscle were largely recapitulated in the EDL and soleus (Figure S1) and highlight the global effect of acute activation of CRHR2 on skeletal muscle gene transcription regardless of the fiber type composition. Interestingly, Compound B acutely increased the expression of the oxidative MyHC *Myh6* and *Myh7* only in slow-twitch soleus muscle (Figure S1), and not glycolytic TA or EDL. Collectively, these results show that in chow-fed lean mice, UCN2 treatment acutely induces the expression of exercise-responsive genes involved in hypertrophy and metabolism.

### Chronic treatment with a modified UCN2 peptide preserves muscle function during casting immobilization

UCN2 treatment modulates a range of genes and proteins that mediate hypertrophy to ultimately increase skeletal muscle mass. We next determined whether these compounds protect against inactivity-induced skeletal muscle wasting and loss of strength. Lean chow-fed mice were subjected to hindlimb cast immobilization, and force production of the gastrocnemius muscle was assessed *in vivo* after a 14 day treatment with Compound A. Casting decreased maximum force (Figure S2A) and specific force (Figure S2B) produced by gastrocnemius muscle in vehicle-treated mice. Conversely, Compound A treatment increased maximum force (Figure S2A) and specific force (Figure S2B) produced by gastrocnemius muscle in cast-immobilized mice, which was accompanied by an increase in muscle mass (Figure S2C and S2D). These results highlight the efficacy of UCN2 treatment to preserve skeletal muscle function and prevent disuse-induced atrophy.

To assess the effects of UCN2 on gene expression following casting, mice were subjected to the same casting protocol as described earlier, but they were only acutely dosed with Compound A or vehicle 6 h prior to sacrifice. Consistent with the acute UCN2 gene data (Figure 4), acute treatment with Compound A after casting had similar effects on gene expression in both gastrocnemius and soleus muscles (Figure S2E and S2F). Acute treatment with UCN2 significantly increased the expression of *Ppargc1a*, *Nr4a2*, *Nr4a3*, and *Trim63* (*MuRF1*) mRNA in both muscle types. In addition, acute treatment with Compound A also increased expression of *Cdkn1*, *Fkbp5*, *Hbegf*, and *Ifrd1* genes that are involved in cell cycle and muscle growth or inhibition of atrophic pathways. These data confirm that acute treatment with UCN2 activates muscle growth pathways while blocking atrophic pathways.

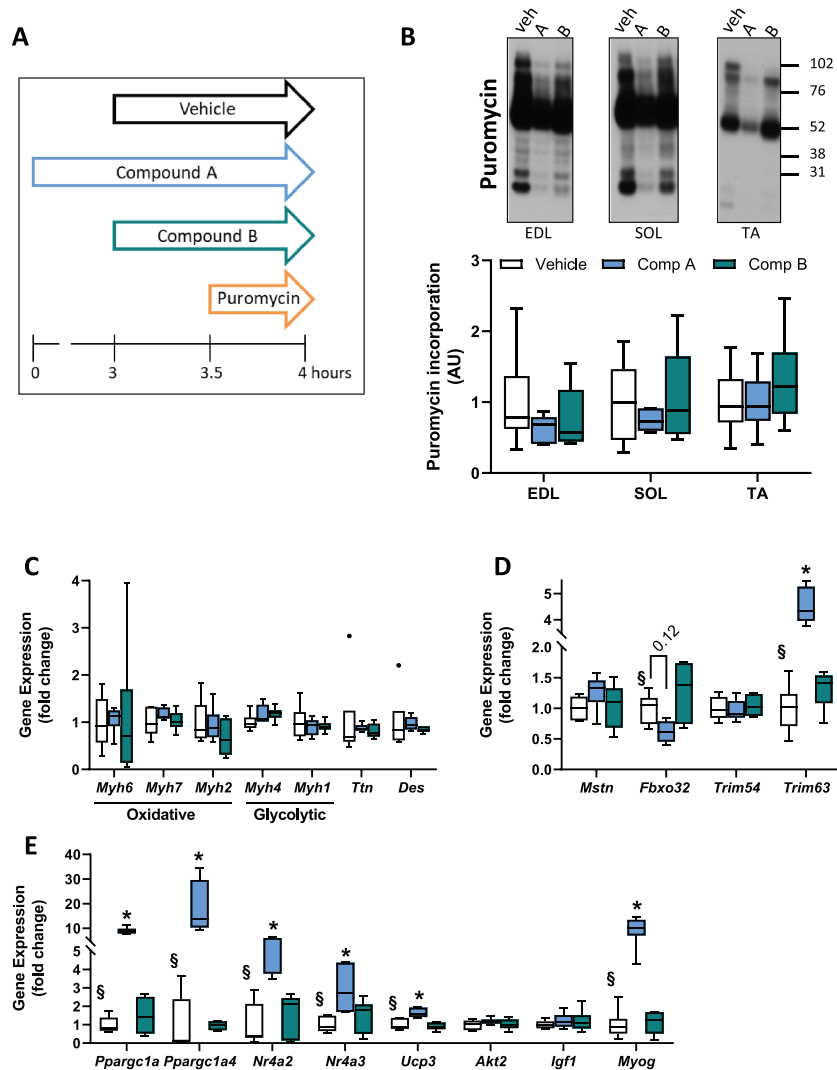


**Figure 4** UCN2 acutely increases transcription factors mediating hypertrophy while rates of protein synthesis remain unchanged in skeletal muscle. (A) Schematic of acute injection experiments. Mice were fasted from 0 to 4 h. (B) *In vivo* muscle protein synthesis determined by puromycin-labeled proteins in chow-fed lean mice after acute Compound A or B injection assessed via the SuNET method. Gene expression data were assessed via qPCR analysis of mRNA from the *tibialis anterior* (TA) after acute Compound A or B injection, (C) structural protein genes, (D) pro-degradation genes, and (E) pro-hypertrophy genes. Results are expressed relative to vehicle-injected mice and normalized to the geometric mean of *Hprt* and *Tbp*.  $n = 6$  mice per group.  $^{\S}P < 0.05$  effect as assessed via one-way analysis of variance or Kruskal–Wallis test,  $^*P < 0.05$  versus vehicle as assessed via *post hoc* analysis.

### Chronic treatment with modified UCN2 peptides improves muscle function in high-fat diet-induced obesity

We next determined whether the increase in skeletal muscle mass in the UCN2 peptide-treated obese mice improves skeletal muscle function. EDL muscle was excised from Compound A-treated or Compound B-treated HFD-fed mice and subjected to fatigue-inducing contractions *ex vivo*. Despite greater skeletal muscle mass (Figure 1), contraction force curves of EDL muscle during fatigue-inducing

stimulation were similar between Compound A-treated and vehicle-treated mice (Figure 5A and 5B). Time to fatigue (Figure 5C) and maximum force production (Figure 5D) of EDL and glycogen content of TA muscle (Figure 5E) were unaltered despite the increased muscle mass between Compound A-treated and vehicle-treated mice. Conversely, muscles from Compound B-treated mice showed functional changes in force generation. Contraction force curves of EDL muscle from Compound B-treated mice were greater during fatigue-inducing contractions, when expressed as either absolute force or percentage of starting force as compared with vehicle-treated mice (Figure 5A and 5B). EDL muscle from

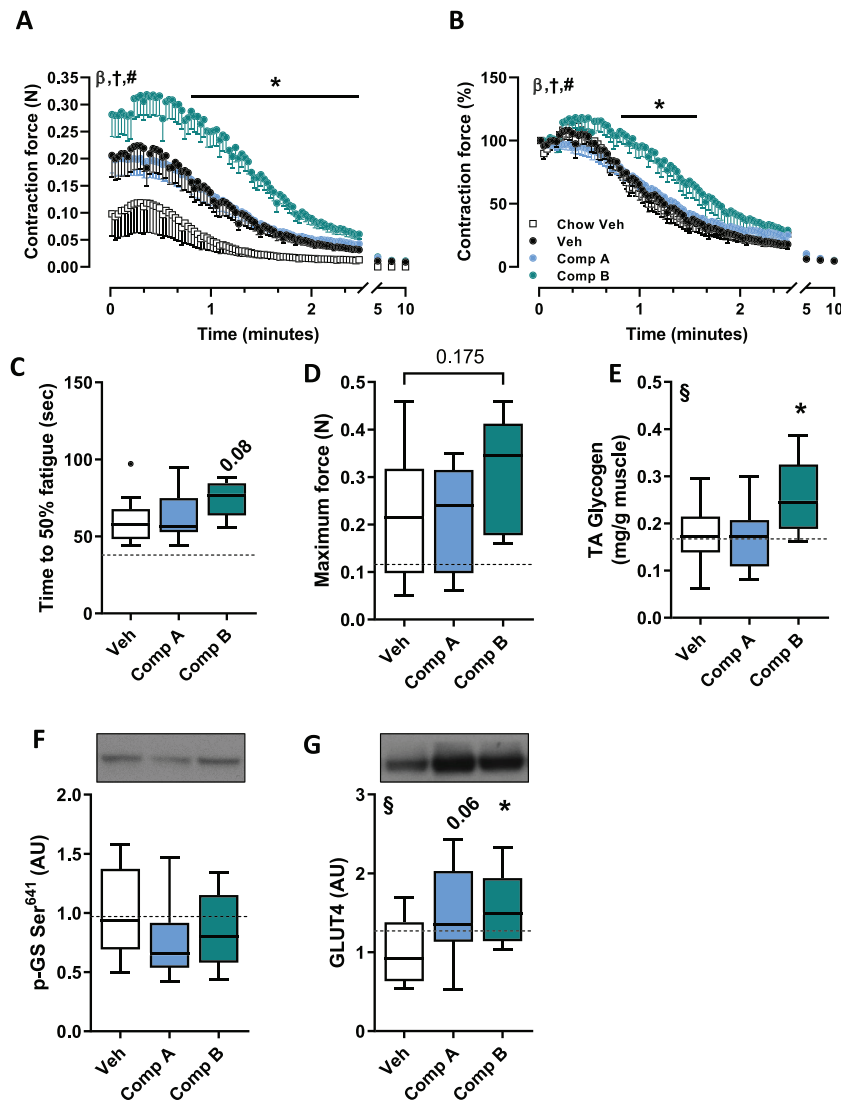


**Figure 5** UCN2 treatment leads to improved skeletal muscle function during *ex vivo* contractions in HFD-fed mice. At the end of 14 days of compound treatment in HFD-fed mice, the EDL muscle was excised and subjected to electrical stimulation and contracted with a fatigue-inducing protocol for 10 min for measurement of (A) absolute force and (B) relative force production during *ex vivo* contractions (electrical stimulation with 100 Hz, 0.2 ms pulse duration, 20 V at a rate of 0.2 s contraction every 2 s, while contralateral muscles were kept under resting passive tension conditions).  $\beta$ Main effect for Compound B treatment.  $\dagger$ Main effect for time.  $\#$ Interaction. \*Compound B versus vehicle control as assessed via two-way repeated measures analysis of variance with Sidak's *post hoc* analysis. (C) Time to 50% fatigue and (D) maximum force produced in EDL. (E) Glycogen content, (F) glycogen synthase phosphorylation at Ser<sup>641</sup>, and (G) total GLUT4 protein content in *tibialis anterior* (TA). Dotted line indicates the mean of chow vehicle mice.  $n = 9$ –10 HFD-fed mice per group.  $\S P < 0.05$  effect as assessed via one-way analysis of variance or Kruskal–Wallis test,  $*P < 0.05$  versus vehicle as assessed via *post hoc* analysis.

Compound B-treated mice was more fatigue resistant, with greater time to fatigue (Figure 5C) and a trend for increased maximal force production (Figure 5D), as compared with EDL from vehicle-treated mice. This 'fatigue resistance' may be due to increased substrate availability, given that glycogen content in TA muscle was greater in Compound B-treated versus vehicle-treated mice (Figure 5E). Phosphorylation of glycogen synthase (Figure 5F) was unchanged, while GLUT4 abundance was increased by similar amounts with both Compound A and B treatment (Figure 5H).

### Chronic treatment with modified UCN2 peptides does not alter contraction-induced glucose uptake

Immediately following fatigue-inducing contractions, glucose uptake was determined in EDL muscle from Compound A-treated or Compound B-treated HFD-fed mice. Contractions *per se* increased glucose uptake in EDL muscle from all mice, but there was no further increase in response to Compound A or B treatment (Figure 6A). AMPK signaling is a possible mediator of CRHR2 activation.<sup>35,36</sup> We found that

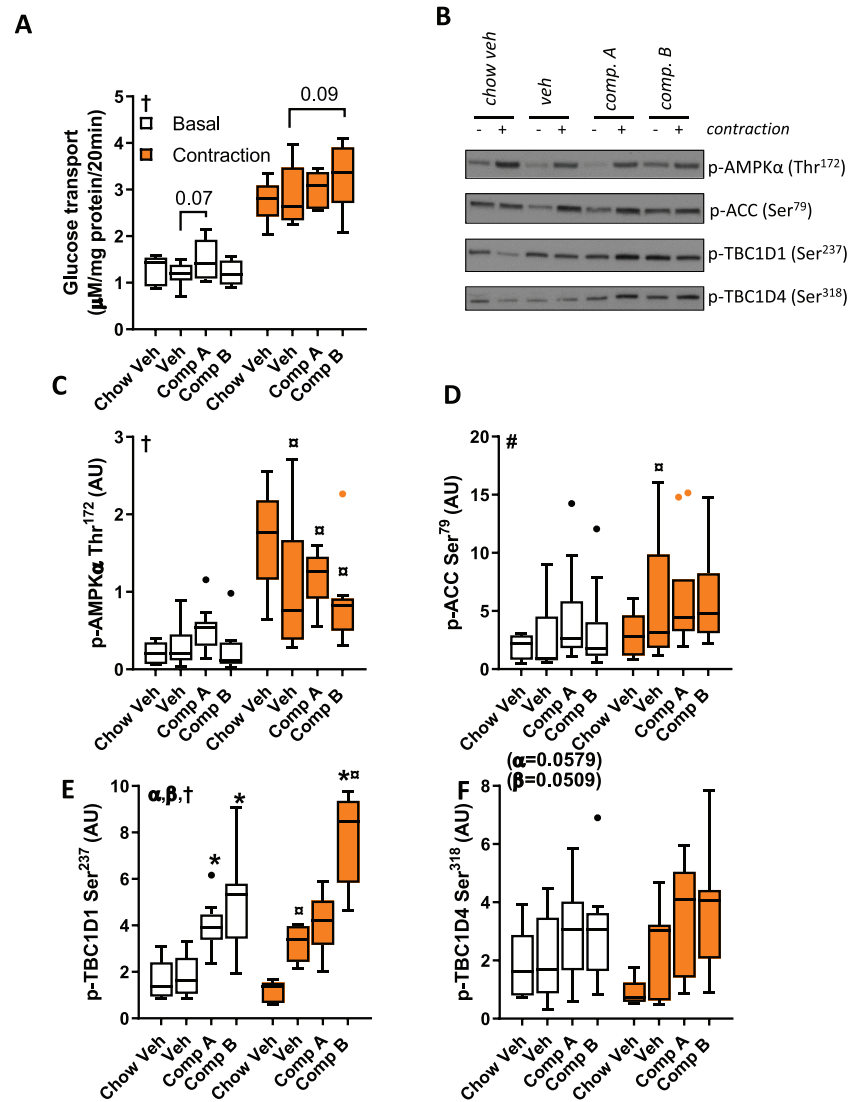


**Figure 6** UCN2 treatment does not alter contraction-induced glucose transport but increases TBC1D1 phosphorylation. Immediately following fatigue-inducing contractions, glucose uptake and signaling was determined in EDL muscle. (A) Contraction-induced glucose uptake assessed with radioactive labeled glucose. (B) Representative western blots. Quantification of (C) p-AMPK $\alpha$  Thr<sup>172</sup>, (D) p-ACC Ser<sup>79</sup>, (E) TBC1D1 phosphorylation at Ser<sup>237</sup>, and (F) TBC1D4 phosphorylation at Ser<sup>318</sup>,  $n = 5$  chow-fed and  $n = 9$ – $10$  HFD-fed mice per group. <sup>†</sup> $P < 0.05$  main effect for Compound A treatment. <sup>‡</sup>Main effect for Compound B treatment. <sup>††</sup> $P < 0.05$  main effect for contraction. <sup>\*</sup> $P < 0.05$  interaction. <sup>#</sup>Compared with vehicle of same condition. <sup>‡‡</sup>Compared with basal of the same treatment as assessed via two-way repeated measures analysis of variance with Sidak's *post hoc* analysis.

phosphorylation of AMPK $\alpha$  (Figure 6B and 6C) and ACC, a downstream target of AMPK (Figure 6D), was unchanged in skeletal muscle from either Compound A-treated or B-treated mice. The Rab-GTPase-activating proteins TBC1D1 and TBC1D4 play critical roles in GLUT4 translocation and glucose transport in skeletal muscle.<sup>37,38</sup> Phosphorylation status of TBC1D1 and TBC1D4 was assessed after fatigue-inducing contractions. Phosphorylation of TBC1D1 was increased under basal conditions in skeletal muscle from either Compound A-treated or B-treated mice as compared with vehicle-treated controls and was further increased by contractions in EDL muscle from Compound B-treated mice (Figure 6E). Although not reaching significance, a trend for

increased TBC1D4 phosphorylation was observed in skeletal muscle from either Compound A-treated or B-treated mice as compared with vehicle-treated controls (Figure 6F). Collectively, these results suggest that both Compound A and B treatment increases TBC1D1 phosphorylation.

### *Chronic treatment with modified UCN2 peptides improves lean mass and skeletal muscle protein synthesis in ob/ob mice*

We determined the effects of Compound A or B treatment for 14 days on skeletal muscle mass and protein synthesis

in the *ob/ob* mouse, a leptin-deficient mouse model that develops severe obesity, and aggravated the loss of skeletal muscle mass.<sup>27</sup> Vehicle-treated *ob/ob* mice gained  $2.16 \pm 0.26$  g of body weight over the 14 day treatment period, while Compound A-treated mice lost  $1.95 \pm 0.29$  g of body weight. Conversely, Compound B-treated mice gained  $2.85 \pm 0.22$  g of body weight (Figure 7A). Based on these

notable changes in body weight, the magnetic resonance imaging results are expressed as the change over the treatment period as a percentage of total body weight. Compound A-treated and Compound B-treated *ob/ob* mice lost fat mass over the treatment period (Figure 7B), while gaining lean mass (Figure 7C). While the *ob/ob* mice have severe skeletal muscle atrophy as compared with wild-type mice

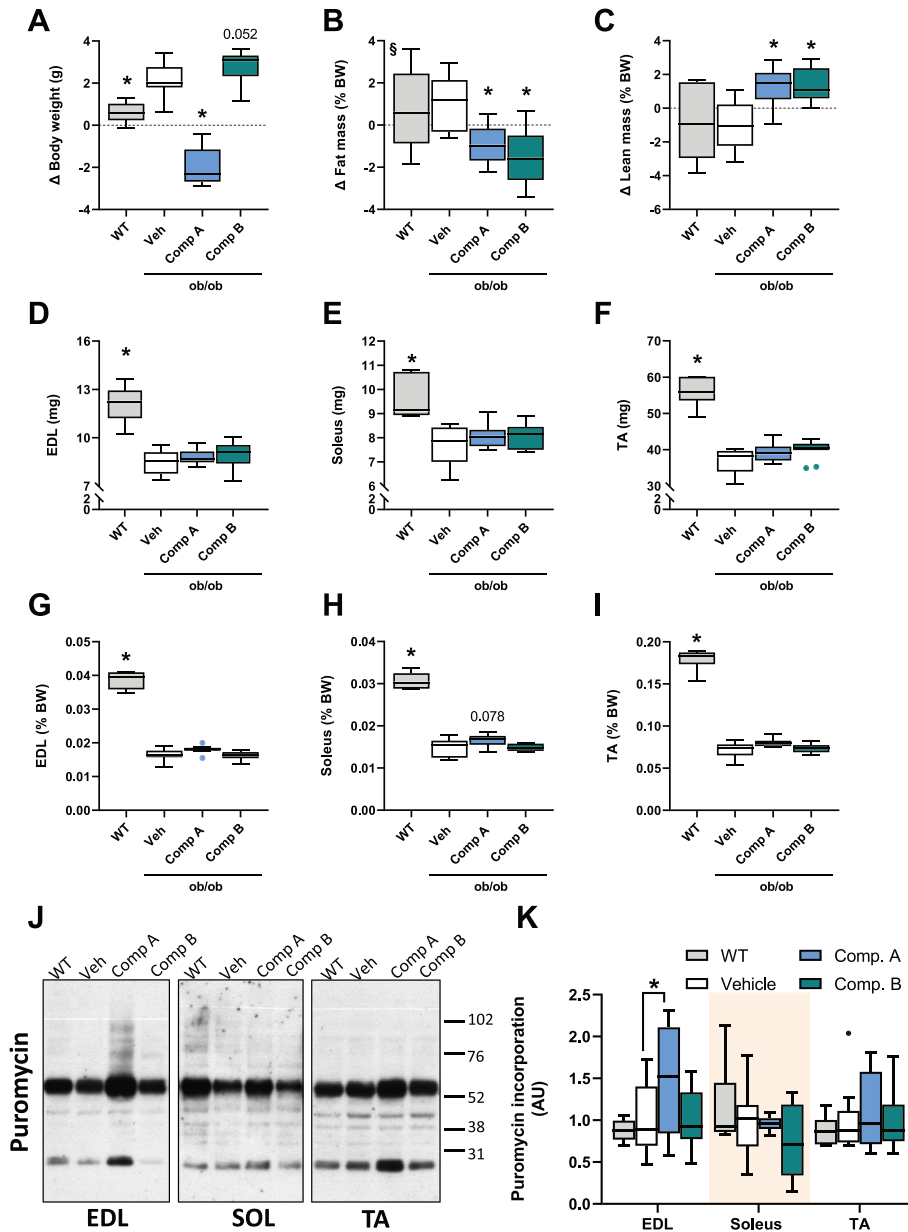


**Figure 7** UCN2 treatment increases lean mass and skeletal muscle protein synthesis in *ob/ob* mice. *ob/ob* mice were treated with vehicle, Compound A, or Compound B for 14 days. Wild-type (WT) mice were treated with vehicle. (A) Change in body weight over the 14 day treatment period. Change in (B) fat mass and (C) lean mass over the 14 day treatment period expressed as a percentage of body weight, assessed with EchoMRI. Absolute weight of (D) extensor digitorum longus (EDL), (E) soleus, and (F) tibialis anterior (TA) muscles. Skeletal muscle weights expressed as percentage of body weight for (G) EDL, (H) soleus, and (I) TA muscles. *In vivo* muscle protein synthesis determined by puromycin-labeled proteins in WT and *ob/ob* mice after the final compound injection, as assessed via the SUNSET method in 4 h fasted mice. (J) Representative western blots and (K) quantification of puromycin-labelled proteins.  $n = 6$  WT,  $n = 9$  Veh,  $n = 9$  Comp. A,  $n = 11$  Comp. B. \* $P < 0.05$  compared with vehicle as assessed via one-way analysis of variance or Kruskal–Wallis test.

(Figure 7D–7I), skeletal muscle weight was not altered after the treatment protocol when expressed as either absolute weights (Figure 7D–7F) or percentage of body weight (Figure 7G–7I). Compound A increased *in vivo* protein synthesis in EDL, but not soleus or TA muscle of ob/ob mice (Figure 7J and 7K).

## Discussion

We have previously demonstrated that Compound A treatment reduces body weight and improves whole-body glucose metabolism by increasing skeletal muscle insulin sensitivity in diet-induced obesity.<sup>25</sup> In the present report, we studied high-fat-fed mice (C57Bl/6J; 26 weeks old) and ob/ob mice (11 weeks old), as well as a separate group of chow-fed C57Bl/6J mice (12 weeks old) subjected to hindlimb cast immobilization. In all three models, we provide evidence that modified UCN2 peptides preserve skeletal muscle mass and function in diet-induced obese and leptin-deficient ob/ob mice, as well as during casting immobilization. Here, we show that treatment of high-fat-fed mice for 14 days with Compound A increases skeletal muscle mass relative to body weight, with a potential fiber type transformation favoring fast-twitch, glycolytic fibers, and an activation of both anabolic (p-S6) and catabolic (MAFbx, p-ULK) pathways. A single Compound A injection increases the expression of a range of genes that are also increased with exercise, while Compound A treatment prevents *in vivo* skeletal muscle force production loss from disuse due to casting. Conversely, Compound B treatment increases skeletal muscle mass only when combined with free wheel running, concomitant with increased glycogen storage and muscle function improvements including skeletal muscle fatigue resistance during *ex vivo* contractions. The distinct pharmacokinetic properties of the compounds may account for the differences in these treatment outcomes. We also show that both Compound A and B treatment in ob/ob mice prevents the loss of skeletal muscle mass, whereas Compound A treatment increases skeletal muscle protein synthesis. Based on our previous data regarding the potencies of the compounds,<sup>25</sup> we speculate that the differences between the compounds are based on half-life and receptor affinity, with the PEGylated compound (Compound A) having a greater capacity to generate cAMP than the non-PEGylated one (Compound B). These results establish modified human UCN2 peptides as viable pharmaceuticals in the treatment of musculoskeletal disorders present in obesity.

The beneficial effects of physical activity are varied and include maintaining healthy metabolism via proper glycemic control and preserving muscle strength to ensure appropriate musculoskeletal function.<sup>10</sup> Unfortunately, exercise can be

impractical or inefficient for those with reduced functional capacity. Here, we show a pharmacological means to simultaneously improve skeletal muscle insulin sensitivity<sup>25</sup> and skeletal muscle function. A plethora of hormones and growth factors can drive skeletal muscle hypertrophy. Signaling through IGF-1 to activate the PI3K–AKT pathway leads to muscle hypertrophy and increased glucose uptake.<sup>39–41</sup> As such, *Igf1* expression is up-regulated in skeletal muscle after chronic UCN2 treatment, leading to increased basal S6 activation. UCN2 peptides also directly induce basal and insulin-stimulated AKT and mTOR phosphorylation *ex vivo*,<sup>25</sup> suggesting signal transduction via the PI3K–AKT–mTOR pathways. Although the exact signaling pathway downstream of CRHR2 is unknown, skeletal muscle mass is not increased in response to sauvagine (UCN1 orthologue that binds to both CRHR1 and CRHR2) after denervation in CRHR2-knockout mice, indicating that CRHR2 signaling is required for gains in skeletal muscle mass.<sup>22</sup> CRHR2 signaling also appears to increase cAMP,<sup>22</sup> which through PKA could increase insulin-stimulated AKT phosphorylation, while directly inducing mTOR phosphorylation in the absence of insulin.<sup>25</sup> Furthermore, UCN2 acutely up-regulated the splice isoform *PGC1 $\alpha$ 4*, which is induced by resistance exercise and increases *Igf1* to promote hypertrophy of skeletal muscle.<sup>42</sup> Additionally, *NR4a2* and *NR4a3* were induced acutely in skeletal muscle by UCN2. These members of the nuclear receptor superfamily can be induced by a single exercise bout<sup>43</sup> and via mTOR signaling leads to skeletal muscle hypertrophy.<sup>44</sup> Modified UCN2 peptides increase the expression of a range of genes that lead to PI3K–AKT–mTOR pathway activation and skeletal muscle hypertrophy, although the physiological importance of these different molecular triggers warrants further investigation.

Signaling through the PI3K–AKT–mTOR axis is pivotal for skeletal muscle differentiation and growth. For example, constitutively active AKT is sufficient to induce skeletal muscle hypertrophy.<sup>45,46</sup> Treating mice with Compound A increases AKT protein abundance in EDL muscle<sup>25</sup> and sustains basal activation of phosphorylated S6 in TA muscle, suggesting increased protein synthesis rates. Compound A treatment did not acutely affect *in vivo* protein synthesis as assessed via SUnSET, an unexpected result given the long-term gains in skeletal muscle mass and activation signaling to protein synthesis after 14 days of treatment. These effects may either represent a difference in temporal signaling through CRHR2 or suggest that any long-term changes in protein synthesis may be caused by the acute transcriptional network activation, which seems likely given that a 14 day Compound A treatment increased protein synthesis in skeletal muscle of ob/ob mice. Furthermore, viral delivery of *UCN2* reduced protein synthesis in liver,<sup>47</sup> while producing a metabolic favorable phenotype. We also observed that the abundance of the pro-atrophy MAFbx was restored to the levels in chow-fed mice, concomitant with activation of FOXO1, which

would normally switch off its expression.<sup>34,48</sup> MAFbx is essential for tissue remodelling in skeletal muscle hypertrophy.<sup>49</sup> The expression of *Trim63* (MuRF1) was reduced with Compound B treatment, which can cause muscle atrophy through Titin degradation.<sup>50</sup> These mild effects could contribute to the increased skeletal muscle mass with UCN2 treatment. Furthermore, ULK1 was activated in skeletal muscle after UCN2 treatment, which is beneficial for hypertrophy by inhibiting apoptosis and promoting normal autophagy.<sup>51</sup> Signaling through IGF-1 and AKT leads to increased expression of myogenin (MYOG), a transcription factor specific to skeletal muscle, which is an important marker of differentiation.<sup>52</sup> *Myog* mRNA was increased in response to acute UCN2 injection. Modified UCN2 peptides activate a range of transcriptional pathways that mediate both skeletal muscle protein synthesis and degradation, highlighting the complex mechanism of UCN2-induced skeletal muscle hypertrophy.

Obesity is often characterized by preferential atrophy of glycolytic type II muscle fibres,<sup>5,53</sup> which can be rescued with exercise training.<sup>54</sup> Here, we suggest that a 14 day treatment with UCN2 peptides in obese mice results in a fiber type transformation from oxidative to glycolytic fibers. This fiber type transformation is not entirely unexpected, as CRHR2 activation through global UCN3 overexpression in mice exhibit a shift towards type II glycolytic fibers.<sup>19</sup> Intriguingly, a similar change is also observed in NR4a3 transgenic mice, where a shift from type I and type IIb towards type IIa and type IIx fibers occurs,<sup>55</sup> while PGC1- $\alpha$ 4 transgenic mice show hypertrophy and a fiber type switch from IIb to IIa and IIx fibers.<sup>42</sup> Conversely, skeletal muscle-specific IGF-1 transgenic mice exhibit hypertrophy of the EDL muscle, with a shift from type IIa to type IIb fibers.<sup>56</sup> The fatigue-resistant NR4a3 transgenic mice are also characterized by improvements in skeletal muscle autophagy and hypertrophy through mTOR signaling.<sup>44</sup> Although the experiments included in the present study were not conducted in aged mice, they were carried out in obese, insulin-resistant mice. Given that aging is associated with insulin resistance,<sup>4</sup> the modified UCN2 peptides used in this study may also be effective in aged, obese mice. Notably, we confirmed the therapeutic nature of UCN2 peptides to mitigate the loss of skeletal muscle mass associated with obesity.<sup>27</sup>

We have previously shown that insulin-stimulated glucose uptake is increased in skeletal muscles from Compound A-treated mice.<sup>25</sup> This metabolic response did not translate into an increase in glycogen storage, suggesting enhanced glucose oxidation. Compound B treatment increased glycogen content, which is also evident in skeletal muscle of UCN3 transgenic mice.<sup>19</sup> Increased glycogen synthesis and storage is a characteristic feature of many mouse models, including IGF-1 treatment<sup>57</sup> and UCN3 overexpression,<sup>19</sup> which also phenocopies UCN2 peptide-treated mice. Furthermore, overexpression of IGF-1 in skeletal muscle results in a preference for glycolytic metabolism,<sup>58</sup> which can increase insulin

sensitivity and improve body composition.<sup>4,10</sup> While the discrepancies between Compound A and B treatment are difficult to explain, different ligands signaling through the same G protein-coupled receptor may have distinct downstream effects. Signalling through CRHR1 or 2 by UCN1 leads to phosphorylation of MAP-kinase and CREB, whereas the binding of CRF does not.<sup>59,60</sup> Different ligands can fine-tune downstream signaling to mediate specific effects on growth and metabolism.

Exercise training programmes in individuals with sarcopenic obesity are beneficial to reduce frailty and preserve lean mass.<sup>4,61</sup> Physiological loss of skeletal muscle mass and force production that occurs in models of chronic disease and disuse can be prevented by treating mice systemically with UCN2.<sup>20,23,24</sup> In the current study, Compound B treatment of obese mice increased the time to fatigue in the EDL muscle without altering its mass, while Compound A treatment increased skeletal muscle mass and preserved force production after casting in chow-fed mice. The greater muscle mass of the EDL did not translate to increased time to fatigue in Compound A-treated mice. This may be due to higher glycogen levels in skeletal muscle from Compound B-treated mice, potentially increasing substrate availability for the contracting fast-twitch type IIx fibers. Furthermore, changes in mitochondrial density do not appear to account for the fatigue resistance, as citrate synthase (a proxy for mitochondrial density) was unchanged by UCN2 treatment (data not shown). Differences in bioenergetics between Compound A and Compound B treatment may be methodologically accounted for by differences in diet (normal chow vs. HFD), the mode of contraction stimulation (*in vivo* tibial nerve stimulation vs. *ex vivo* direct electrical stimulation), and the specific electrical protocol used (force/frequency curve vs. fatigue-inducing stimulation). UCN2 peptide treatment has numerous beneficial effects on the functional properties of skeletal muscle.

Exercise/muscle contractions increase glucose uptake by an insulin-independent manner and are considered an important physiological process to promote glucose uptake in insulin-resistant skeletal muscle.<sup>4,10</sup> We have previously reported that Compound A increased insulin-stimulated glucose uptake in skeletal muscle of HFD-fed mice.<sup>25</sup> Here, we investigated if UCN2 treatment could also increase contraction-induced glucose uptake in skeletal muscle from obese, insulin-resistant mice. While contractions *per se* increased glucose transport in skeletal muscle, UCN2 treatment did not elicit any further effect. We used a fatigue-inducing contraction protocol, which may have masked more subtle changes in metabolic properties as the muscles are in high energy demand and different contraction protocols can affect the rates of glucose uptake.<sup>62</sup> Furthermore, UCN2 treatment increased TBC1D1 phosphorylation, a key component of contraction-induced GLUT4 translocation,<sup>38</sup> in EDL muscle studied under basal conditions and in response to

contraction, suggesting an overall improvement in the components governing GLUT4 translocation and glucose uptake. TBC1D1/TBC1D4 phosphorylation is necessary but not sufficient for GLUT4 translocation.<sup>63</sup> We also found that Compound A and Compound B treatment increased total GLUT4 abundance in EDL muscle. We have previously reported that Compound A increases GLUT4 trafficking to the sarcolemma membrane.<sup>25</sup> Different pools of GLUT4 vesicles respond selectively to insulin or muscle contraction,<sup>64</sup> such that contraction depletes GLUT4 from transferrin receptor-positive endosomes that are not affected by insulin,<sup>65,66</sup> while GLUT4 trafficking to the membrane is additive in response to a combined stimulation with insulin and contraction.<sup>67,68</sup> An increase in total abundance of GLUT4 may not translate to an increase in either insulin or contraction-induced glucose uptake.

The vast beneficial effects of exercise are often unattainable for frail and elderly individuals, as well as for individuals with obesity, and as such, there is growing interest to identify and develop specific compounds that activate different cellular targets induced by exercise to improve functional properties of skeletal muscle. While we report positive effects of UCN2 peptides on muscle mass and function, future studies are warranted to ascertain whether the compounds will act identically in older wild-type mice. Our results indicate that UCN2 peptides improve muscle mass and function, making UCN2 peptides durable candidates for the treatment of musculoskeletal disorders.

## Acknowledgements

The authors of this manuscript certify that they comply with the ethical guidelines for authorship and publishing in the *Journal of Cachexia, Sarcopenia and Muscle*. The authors are thankful to Ann-Marie Pettersson, Torbjörn Morein, and

Katrin Ingermo (Section for Integrative Physiology, Karolinska Institutet, Sweden) for technical assistance.

## Conflict of interest

J.A.F., B.Y., A.C., and J.T.B. are employees of Eli Lilly and Company. J.R.Z. received Compounds A and B as a gift from Eli Lilly and Company. No other potential conflicts of interest relevant to this article were reported.

## Funding

Vetenskapsrådet (Swedish Research Council) (2015-00165, 2019-01282), Swedish Diabetes Foundation (DIA2018-357, DIA2019-451), Novo Nordisk Foundation (NNF17OC0030088), and Strategic Research Programme in Diabetes at Karolinska Institutet (Swedish Research Council grant number 2009-1068) supported this research. M.L.B. was supported by the Swedish Society for Medical Research.

## Author contributions

M.L.B., H.K.R.K., J.T.B., and J.R.Z. designed the study. M.L.B., J.M., T.D.C.B., A.A.O., J.A.B.S., J.A.F., B.Y., A.E.C., and H.K.R.K. researched data. M.L.B., J.M., J.T.B., and J.R.Z. analysed and interpreted the data. J.M., J.T.L., and J.T.B. contributed to discussion and reviewed/edited the manuscript. The manuscript was written by M.L.B., J.T.B., and J.R.Z. and approved by all authors. J.R.Z. is the guarantor of this work and, as such, had full access to all the data in the study and take responsibility for the integrity of the data and the accuracy of the analysis.

## References

1. Organization WH. Geneva. Global report on diabetes <http://www.who.int/diabetes/global-report/en/> 2006.
2. Narici MV, Maffulli N. Sarcopenia: characteristics, mechanisms and functional significance. *Br Med Bull* 2010;**95**:139–159.
3. Stenholm S, Harris TB, Rantanen T, Visser M, Kritchevsky SB, Ferrucci L. Sarcopenic obesity: definition, cause and consequences. *Curr Opin Clin Nutr Metab Care* 2008;**11**:693–700.
4. Cartee GD, Hepple RT, Bamman MM, Zierath JR. Exercise promotes healthy aging of skeletal muscle. *Cell Metab* 2016;**23**:1034–1047.
5. Vandervoort AA. Aging of the human neuromuscular system. *Muscle Nerve* 2002;**25**:17–25.
6. Solomon AM, Bouloux PM. Modifying muscle mass—the endocrine perspective. *J Endocrinol* 2006;**191**:349–360.
7. Dreyer HC, Volpi E. Role of protein and amino acids in the pathophysiology and treatment of sarcopenia. *J Am Coll Nutr* 2005;**24**:140S–145S.
8. Szulc P, Duboeuf F, Marchand F, Delmas PD. Hormonal and lifestyle determinants of appendicular skeletal muscle mass in men: the MINOS study. *Am J Clin Nutr* 2004;**80**:496–503.
9. Roth SM, Metter EJ, Ling S, Ferrucci L. Inflammatory factors in age-related muscle wasting. *Curr Opin Rheumatol* 2006;**18**:625–630.
10. Egan B, Zierath JR. Exercise metabolism and the molecular regulation of skeletal muscle adaptation. *Cell Metab* 2013;**17**:162–184.
11. Walczewska J, Dzieza-Grudnik A, Siga O, Grodzicki T. The role of urocortins in the cardiovascular system. *J Physiol Pharmacol* 2014;**65**:753–766.
12. Kuperman Y, Chen A. Urocortins: emerging metabolic and energy homeostasis

- perspectives. *Trends Endocrinol Metab* 2008;**19**:122–129.
13. Broberger C. Brain regulation of food intake and appetite: molecules and networks. *J Intern Med* 2005;**258**:301–327.
  14. Chen A, Blount A, Vaughan J, Brar B, Vale W. Urocortin II gene is highly expressed in mouse skin and skeletal muscle tissues: localization, basal expression in corticotropin-releasing factor receptor (CRFR) 1- and CRFR2-null mice, and regulation by glucocorticoids. *Endocrinology* 2004;**145**:2445–2457.
  15. Kishimoto T, Pearce RV 2nd, Lin CR, Rosenfeld MG. A sauvagine/corticotropin-releasing factor receptor expressed in heart and skeletal muscle. *Proc Natl Acad Sci U S A* 1995;**92**:1108–1112.
  16. Lovenberg TW, Chalmers DT, Liu C, De Souza EB. CRF2 alpha and CRF2 beta receptor mRNAs are differentially distributed between the rat central nervous system and peripheral tissues. *Endocrinology* 1995;**136**:4139–4142.
  17. Kuperman Y, Issler O, Vaughan J, Bilezikjian L, Vale W, Chen A. Expression and regulation of corticotropin-releasing factor receptor type 2 $\beta$  in developing and mature mouse skeletal muscle. *Mol Endocrinol* 2011;**25**:157–169.
  18. Bale TL, Anderson KR, Roberts AJ, Lee KF, Nagy TR, Vale WW. Corticotropin-releasing factor receptor-2-deficient mice display abnormal homeostatic responses to challenges of increased dietary fat and cold. *Endocrinology* 2003;**144**:2580–2587.
  19. Jamieson PM, Cleasby ME, Kuperman Y, Morton NM, Kelly PA, Brownstein DG, et al. Urocortin 3 transgenic mice exhibit a metabolically favourable phenotype resisting obesity and hyperglycaemia on a high-fat diet. *Diabetologia* 2011;**54**:2392–2403.
  20. Hinkle RT, Donnelly E, Cody DB, Bauer MB, Isfort RJ. Urocortin II treatment reduces skeletal muscle mass and function loss during atrophy and increases nonatrophying skeletal muscle mass and function. *Endocrinology* 2003;**144**:4939–4946.
  21. Hinkle RT, Donnelly E, Cody DB, Bauer MB, Sheldon RJ, Isfort RJ. Corticotropin releasing factor 2 receptor agonists reduce the denervation-induced loss of rat skeletal muscle mass and force and increase non-atrophying skeletal muscle mass and force. *J Muscle Res Cell Motil* 2004;**25**:539–547.
  22. Hinkle RT, Donnelly E, Cody DB, Samuelsson S, Lange JS, Bauer MB, et al. Activation of the CRF 2 receptor modulates skeletal muscle mass under physiological and pathological conditions. *Am J Physiol Endocrinol Metab* 2003;**285**:E889–E898.
  23. Hinkle RT, Lefever FR, Dolan ET, Reichart DL, Dietrich JA, Gropp KE, et al. Corticotropin releasing factor 2 receptor agonist treatment significantly slows disease progression in mdx mice. *BMC Med* 2007;**5**:18.
  24. Hinkle RT, Lefever FR, Dolan ET, Reichart DL, Zwolschen JM, Oneill TP, et al. Treatment with a corticotropin releasing factor 2 receptor agonist modulates skeletal muscle mass and force production in aged and chronically ill animals. *BMC Musculoskelet Disord* 2011;**12**:15.
  25. Borg ML, Massart J, Schonke M, De Castro BT, Guo L, Wade M, et al. Modified UCN2 peptide acts as an insulin sensitizer in skeletal muscle of obese mice. *Diabetes* 2019;**68**:1403–1414.
  26. Isfort RJ, Wang F, Tscheiner M, Dolan E, Bauer MB, Lefever F, et al. Modifications of the human urocortin 2 peptide that improve pharmacological properties. *Peptides* 2006;**27**:1806–1813.
  27. Trostler N, Romsos DR, Bergen WG, Leveille GA. Skeletal muscle accretion and turnover in lean and obese (ob/ob) mice. *Metabolism* 1979;**28**:928–933.
  28. Sainz N, Rodriguez A, Catalan V, Becerril S, Ramirez B, Gomez-Ambrosi J, et al. Leptin administration favors muscle mass accretion by decreasing FoxO3a and increasing PGC-1 $\alpha$  in ob/ob mice. *PLoS One* 2009;**4**:e6808.
  29. Schmidt EK, Clavarino G, Ceppi M, Pierre P. SUNSET, a nonradioactive method to monitor protein synthesis. *Nat Methods* 2009;**6**:275–277.
  30. Barres R, Yan J, Egan B, Treebak JT, Rasmussen M, Fritz T, et al. Acute exercise remodels promoter methylation in human skeletal muscle. *Cell Metab* 2012;**15**:405–411.
  31. Hansen PA, Gulve EA, Holloszy JO. Suitability of 2-deoxyglucose for in vitro measurement of glucose transport activity in skeletal muscle. *J Appl Physiol (1985)* 1994;**76**:979–985.
  32. Kulkarni SS, Karlsson HK, Szekeres F, Chibalin AV, Krook A, Zierath JR. Suppression of 5'-nucleotidase enzymes promotes AMP-activated protein kinase (AMPK) phosphorylation and metabolism in human and mouse skeletal muscle. *J Biol Chem* 2011;**286**:34567–34574.
  33. Cleasby ME, Jamieson PM, Atherton PJ. Insulin resistance and sarcopenia: mechanistic links between common co-morbidities. *J Endocrinol* 2016;**229**:R67–R81.
  34. Stitt TN, Drujan D, Clarke BA, Panaro F, Timofeyeva Y, Kline WO, et al. The IGF-1/PI3K/Akt pathway prevents expression of muscle atrophy-induced ubiquitin ligases by inhibiting FOXO transcription factors. *Mol Cell* 2004;**14**:395–403.
  35. Li J, Qi D, Cheng H, Hu X, Miller EJ, Wu X, et al. Urocortin 2 autocrine/paracrine and pharmacologic effects to activate AMP-activated protein kinase in the heart. *Proc Natl Acad Sci U S A* 2013;**110**:16133–16138.
  36. Roustit MM, Vaughan JM, Jamieson PM, Cleasby ME. Urocortin 3 activates AMPK and AKT pathways and enhances glucose disposal in rat skeletal muscle. *J Endocrinol* 2014;**223**:143–154.
  37. Moltke I, Grarup N, Jorgensen ME, Bjerregaard P, Treebak JT, Fumagalli M, et al. A common Greenlandic TBC1D4 variant confers muscle insulin resistance and type 2 diabetes. *Nature* 2014;**512**:190–193.
  38. Peck GR, Chavez JA, Roach WG, Budnik BA, Lane WS, Karlsson HK, et al. Insulin-stimulated phosphorylation of the Rab GTPase-activating protein TBC1D1 regulates GLUT4 translocation. *J Biol Chem* 2009;**284**:30016–30023.
  39. Di Cola G, Cool MH, Accili D. Hypoglycemic effect of insulin-like growth factor-1 in mice lacking insulin receptors. *J Clin Invest* 1997;**99**:2538–2544.
  40. Palazzolo I, Stack C, Kong L, Musaro A, Adachi H, Katsuno M, et al. Overexpression of IGF-1 in muscle attenuates disease in a mouse model of spinal and bulbar muscular atrophy. *Neuron* 2009;**63**:316–328.
  41. Rommel C, Bodine SC, Clarke BA, Rossman R, Nunez L, Stitt TN, et al. Mediation of IGF-1-induced skeletal myotube hypertrophy by PI(3)K/Akt/mTOR and PI(3)K/Akt/GSK3 pathways. *Nat Cell Biol* 2001;**3**:1009–1013.
  42. Ruas JL, White JP, Rao RR, Kleiner S, Brannan KT, Harrison BC, et al. A PGC-1 $\alpha$  isoform induced by resistance training regulates skeletal muscle hypertrophy. *Cell* 2012;**151**:1319–1331.
  43. Mahoney DJ, Parise G, Melov S, Safdar A, Tarnopolsky MA. Analysis of global mRNA expression in human skeletal muscle during recovery from endurance exercise. *FASEB J* 2005;**19**:1498–1500.
  44. Goode JM, Pearen MA, Tuong ZK, Wang SC, Oh TG, Shao EX, et al. The nuclear receptor, Nor-1, induces the physiological responses associated with exercise. *Mol Endocrinol* 2016;**30**:660–676.
  45. Blaauw B, Canato M, Agatea L, Toniolo L, Mammucari C, Masiero E, et al. Inducible activation of Akt increases skeletal muscle mass and force without satellite cell activation. *FASEB J* 2009;**23**:3896–3905.
  46. Pallafacchina G, Calabria E, Serrano AL, Kalhovde JM, Schiaffino S. A protein kinase B-dependent and rapamycin-sensitive pathway controls skeletal muscle growth but not fiber type specification. *Proc Natl Acad Sci U S A* 2002;**99**:9213–9218.
  47. Kim YC, Truax AD, Giamouridis D, Lai NC, Guo T, Hammond HK, et al. Significant alteration of liver metabolites by AAV8. Urocortin 2 gene transfer in mice with insulin resistance. *PLoS One* 2019;**14**:e0224428.
  48. Latres E, Amini AR, Amini AA, Griffiths J, Martin FJ, Wei Y, et al. Insulin-like growth factor-1 (IGF-1) inversely regulates atrophy-induced genes via the phosphatidylinositol 3-kinase/Akt/mammalian target of rapamycin (PI3K/Akt/mTOR) pathway. *J Biol Chem* 2005;**280**:2737–2744.
  49. Baehr LM, Tunzi M, Bodine SC. Muscle hypertrophy is associated with increases in proteasome activity that is independent of MuRF1 and MAFbx expression. *Front Physiol* 2014;**5**:69.
  50. Centner T, Yano J, Kimura E, McElhinny AS, Pelin K, Witt CC, et al. Identification of muscle specific ring finger proteins as potential regulators of the titin kinase domain. *J Mol Biol* 2001;**306**:717–726.
  51. Luo L, Lu AM, Wang Y, Hong A, Chen Y, Hu J, et al. Chronic resistance training activates autophagy and reduces apoptosis

- of muscle cells by modulating IGF-1 and its receptors, Akt/mTOR and Akt/FOXO3a signaling in aged rats. *Exp Gerontol* 2013;**48**:427–436.
52. Musaro A, Rosenthal N. Maturation of the myogenic program is induced by postmitotic expression of insulin-like growth factor I. *Mol Cell Bio* 1999;**19**:3115–3124.
  53. Nair KS. Aging muscle. *Am J Clin Nutr* 2005;**81**:953–963.
  54. Verdijk LB, Gleeson BG, Jonkers RA, Meijer K, Savelberg HH, Dendale P, et al. Skeletal muscle hypertrophy following resistance training is accompanied by a fiber type-specific increase in satellite cell content in elderly men. *J Gerontol A Biol Sci Med Sci* 2009;**64**:332–329.
  55. Pearen MA, Eriksson NA, Fitzsimmons RL, Goode JM, Martel N, Andrikopoulos S, et al. The nuclear receptor, Nor-1, markedly increases type II oxidative muscle fibers and resistance to fatigue. *Mol Endocrinol* 2012;**26**:372–384.
  56. Christoffolete MA, Silva WJ, Ramos GV, Bento MR, Costa MO, Ribeiro MO, et al. Muscle IGF-1-induced skeletal muscle hypertrophy evokes higher insulin sensitivity and carbohydrate use as preferential energy substrate. *Biomed Res Int* 2015;**2015**:282984.
  57. Schmitz F, Hartmann H, Stumpel F, Creutzfeldt W. In vivo metabolic action of insulin-like growth factor I in adult rats. *Diabetologia* 1991;**34**:144–149.
  58. Semsarian C, Wu MJ, Ju YK, Marciniak T, Yeoh T, Allen DG, et al. Skeletal muscle hypertrophy is mediated by a  $Ca^{2+}$ -dependent calcineurin signalling pathway. *Nature* 1999;**400**:576–581.
  59. Grammatopoulos DK, Randeva HS, Levine MA, Katsanou ES, Hillhouse EW. Urocortin, but not corticotropin-releasing hormone (CRH), activates the mitogen-activated protein kinase signal transduction pathway in human pregnant myometrium: an effect mediated via  $R1\alpha$  and  $R2\beta$  CRH receptor subtypes and stimulation of Gq-proteins. *Mol Endocrinol* 2000;**14**:2076–2091.
  60. Rossant CJ, Pinnock RD, Hughes J, Hall MD, McNulty S. Corticotropin-releasing factor type 1 and type 2 $\alpha$  receptors regulate phosphorylation of calcium/cyclic adenosine 3',5'-monophosphate response element-binding protein and activation of p42/p44 mitogen-activated protein kinase. *Endocrinology* 1999;**140**:1525–1536.
  61. Villareal DT, Aguirre L, Gurney AB, Waters DL, Sinacore DR, Colombo E, et al. Aerobic or resistance exercise, or both, in dieting obese older adults. *N Engl J Med* 2017;**376**:1943–1955.
  62. Jensen TE, Sylow L, Rose AJ, Madsen AB, Angin Y, Maarbjerg SJ, et al. Contraction-stimulated glucose transport in muscle is controlled by AMPK and mechanical stress but not sarcoplasmic reticulum  $Ca^{2+}$  release. *Mol Metab* 2014;**3**:742–753.
  63. Stockli J, Davey JR, Hohnen-Behrens C, Xu A, James DE, Ramm G. Regulation of glucose transporter 4 translocation by the Rab guanosine triphosphatase-activating protein AS160/TBC1D4: role of phosphorylation and membrane association. *Mol Endocrinol* 2008;**22**:2703–2715.
  64. Douen AG, Ramlal T, Rastogi S, Bilan PJ, Cartee GD, Vranic M, et al. Exercise induces recruitment of the “insulin-responsive glucose transporter”. Evidence for distinct intracellular insulin- and exercise-recruitable transporter pools in skeletal muscle. *J Biol Chem* 1990;**265**:13427–13430.
  65. Fazakerley DJ, Lawrence SP, Lizunov VA, Cushman SW, Holman GD. A common trafficking route for GLUT4 in cardiomyocytes in response to insulin, contraction and energy-status signalling. *J Cell Sci* 2009;**122**:727–734.
  66. Ploug T, van Deurs B, Ai H, Cushman SW, Ralston E. Analysis of GLUT4 distribution in whole skeletal muscle fibers: identification of distinct storage compartments that are recruited by insulin and muscle contractions. *J Cell Biol* 1998;**142**:1429–1446.
  67. Ploug T, Wojtaszewski J, Kristiansen S, Hespel P, Galbo H, Richter EA. Glucose transport and transporters in muscle giant vesicles: differential effects of insulin and contractions. *Am J Physiol* 1993;**264**:E270–E278.
  68. Gao J, Ren J, Gulve EA, Holloszy JO. Additive effect of contractions and insulin on GLUT-4 translocation into the sarcolemma. *J Appl Physiol (1985)* 1994;**77**:1597–1601.